ARL-TR-8888 ● JAN 2020

DEVCOM ARMY RESEARCH LABORATORY

Overcoming Erroneous Erosion of Electrically Launched Projectiles in ALEGRA Simulations

by W Casey Uhlig, Matthew J Coppinger, Paul R Berning, and Peter T Bartkowski

NOTICES

Disclaimers

The findings in this report are not to be construed as an official Department of the Army position unless so designated by other authorized documents.

Citation of manufacturer's or trade names does not constitute an official endorsement or approval of the use thereof.

Destroy this report when it is no longer needed. Do not return it to the originator.

ARL-TR-8888 ● JAN 2020

Overcoming Erroneous Erosion of Electrically Launched Projectiles in ALEGRA Simulations

W Casey Uhlig, Matthew J Coppinger, Paul R Berning, and Peter T Bartkowski
Weapons and Materials Research Directorate, CCDC Army Research Laboratory

REPORT DOCUMENTATION PAGE

Form Approved
OMB No. 0704-0188

1. REPORT DATE *(DD-MM-YYYY)*	2. REPORT TYPE	3. DATES COVERED (From - To)
January 2020	Technical Report	4 October 2018–1 July 2019

4. TITLE AND SUBTITLE
Overcoming Erroneous Erosion of Electrically Launched Projectiles in ALEGRA Simulations

5a. CONTRACT NUMBER

5b. GRANT NUMBER

5c. PROGRAM ELEMENT NUMBER

6. AUTHOR(S)
W Casey Uhlig, Matthew J Coppinger, Paul R Berning, and Peter T Bartkowski

5d. PROJECT NUMBER

5e. TASK NUMBER

5f. WORK UNIT NUMBER

7. PERFORMING ORGANIZATION NAME(S) AND ADDRESS(ES)
CCDC Army Research Laboratory
ATTN: FCDD-RLW-PA
Aberdeen Proving Ground, MD 21005

8. PERFORMING ORGANIZATION REPORT NUMBER
ARL-TR-8888

9. SPONSORING/MONITORING AGENCY NAME(S) AND ADDRESS(ES)

10. SPONSOR/MONITOR'S ACRONYM(S)

11. SPONSOR/MONITOR'S REPORT NUMBER(S)

12. DISTRIBUTION/AVAILABILITY STATEMENT
Approved for public release; distribution is unlimited.

13. SUPPLEMENTARY NOTES
ORCID IDs: W Casey Uhlig, 0000-0003-1815-0106; Paul R Berning, 0000-00019699-0245

14. ABSTRACT
Hydrocode simulations were used to directly improve and guide the design of an electrothermal research gun capable of firing small projectiles (0.25 g) at hypervelocity. The launch system uses an electrical arc and vaporization from a pointed copper anode with voltages up to 20 kV to produce a rapidly expanding gas as a propellant. The simulations were performed using ALEGRA with barrel expansion, projectile erosion, and velocity profiles as validation benchmarks. Guidance resulting from these benchmarked simulations led to projectile velocity gains of 30%. While the initial simulations reproduced and predicted the velocity profiles extremely well, significant erosion of the projectile occurred in the simulations that was not observed in the experiments. This was a direct result of Eulerian "welding" at the projectile–barrel interface. Several modifications to the simulations were implemented in this study to maintain the success observed in earlier velocity predictions while preserving projectile integrity to overcome erroneous erosion issues.

15. SUBJECT TERMS
hypervelocity projectiles, electrothermal gun, arc, high voltage, vaporization, wire explosion, ALEGRA

16. SECURITY CLASSIFICATION OF:			17. LIMITATION OF ABSTRACT	18. NUMBER OF PAGES	19a. NAME OF RESPONSIBLE PERSON
a. REPORT	b. ABSTRACT	c. THIS PAGE			W Casey Uhlig
Unclassified	Unclassified	Unclassified	UU	22	19b. TELEPHONE NUMBER (Include area code) (410) 278-3997

Contents

List of Figures

Acknowledgments

The authors would like to thank Aaron Bard for experimental insight, Mike Zellner for Photon Doppler Velocimetry guidance, and James Cazamias and John Niederhaus for simulation insights. This work was supported in part by a grant of computer time from the Department of Defense High Performance Computing Modernization Program at the US Army Research Laboratory's Department of Defense Supercomputing Resource Center and the Terminal Ballistics Frontier project.

1. Introduction

An electrothermal research gun capable of firing small aluminum projectiles (~0.25 g) up to 4 km/s has been developed at the US Army Combat Capabilities Development Command Army Research Laboratory.[1,2] Improvement and design were directly guided by 3-D simulations performed using the multiphysics hydrocode ALEGRA with magnetohydrodynamic (MHD) capabilities developed by Sandia National Laboratories.[3] The system consists of a high-voltage capacitor bank, low-inductance copper leads, and a mechanical high-voltage switch connected to the anode of the gun. The aluminum projectile and gun barrel acted as the cathode. The mechanism for launch is an electrical arc and vaporization of a pointed copper anode with voltages up to 20 kV, producing a rapidly expanding gas. Chemical reactions and electromagnetic forces have little contribution. Although small-caliber electrothermal accelerators and other electromagnetic launch systems have been used for some years for laboratory hypervelocity impact and other studies,[4–9] this gun design focused on a simple, low-cost, reproducible, and potentially disposable device to allow impact and MHD validation studies.

Two barrel configurations were used in this study. The initial barrel design (referred to in this work as "standard barrel") used 4340 steel with a 50.8-mm-long, 9.5-mm-diameter chamber. The as-purchased steel rod had a measured Brinell hardness of 207 (equivalent tensile strength of 695 MPa). The copper anode, which provided copper vapor as the working fluid during firing of the gun, consisted of a 6.35-mm-diameter rod with a region of reduced diameter (nominally 3.2 mm) leading to the vaporizing tip (total length of the reduced diameter region of 25.4 mm). The tip was conical with a length-to-base-diameter ratio (L/D) ranging from 2 to 5. A polyethylene sleeve insulated the copper electrode and epoxy was used to fill the void surrounding the tip. Figure 1a depicts the assembled electrothermal gun with a standard barrel design (capacitive power supply, switch, and gun mount omitted). The other barrel design, shown in Fig. 1b, reduced the chamber diameter to the barrel bore diameter (4.78 mm) with a length of 20 mm and was constructed of hardened 4340 steel with equivalent tensile strengths of 1400 MPa to 1600 MPa based on hardness testing (Brinell hardness of 415 to 477). The total barrel length and location of the projectile–tip interface was kept constant. Thus, the effective breech face or opening to the chamber was moved approximately 30 mm into the steel barrel assembly.

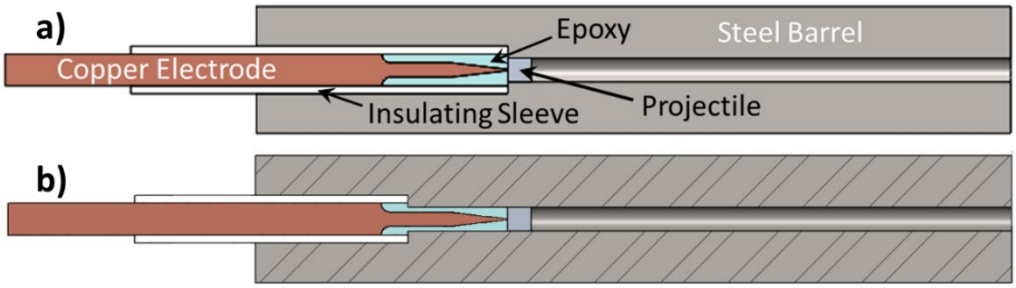

Fig. 1 Illustration of cross section of barrel assembly for two barrel designs: a) standard and b) reduced chamber

The electric launch used a 38-kJ capacitor bank charged to 20 kV. The main metric for the gun was launch velocity, which was characterized using high-speed video, magnetic sensing coils,[10,11] and Photon Doppler Velocimetry (PDV).[12] Additionally, the current through the system and voltage across the gun mount were monitored using a Rogowski coil and 40-kV high-voltage probes, respectively. An electrode tip of L/D 4 was chosen as the standard based on earlier work and all information presented here is based on L/D 4 tips. The standard barrel produced an average peak velocity of 2988 m/s, while the reduced-chamber design resulted in 3850 m/s.

Three benchmarks were used for validation of the ALEGRA simulations. Direct comparisons were made with the velocity profiles from PDV, the measured barrel expansion, and projectile integrity. Guidance resulting from these benchmarked simulations led to strengthening the barrel in the standard design and modifying the chamber; both produced significant projectile velocity gains. While the initial simulations reproduced and predicted the velocity profiles extremely well, significant erosion of the projectile occurred in the simulations that was not observed in the experiments. This was a direct result of Eulerian "welding" at the projectile–barrel interface. Methods solving this interface issue have been implemented in ALEGRA,[13] but that capability is not available for the MHD package required for simulating our electrothermal gun. Several modifications to the simulations were implemented in this study to overcome erroneous erosion issues, preserving projectile integrity, while maintaining the success observed in earlier velocity predictions.

2. Initial ALEGRA Simulations

A cylindrical trisection mesh with one-fourth symmetry was used in the 3-D ALEGRA MHD simulations. The cell edges were less than 0.1 mm in the region of the electrode tip, and a simple elastic–perfectly plastic model with varying yield

strength was used for the steel barrel. The yield strength was chosen based on Brinell-hardness measurements made on the barrels. An external circuit was applied to the mesh comprising a 191-μF capacitor, 10.4-Ω resistor, and 340-nH inductor with electrical input going to the copper anode and zero potential at the barrel. The electrical parameters were chosen in the simulation to produce current output similar to nominal experimentally measured current from the standard barrel shots and were not modified throughout the study. The magnitude of the current density, JE, observed in the simulations is shown in Fig. 2 for the standard barrel at 1, 5, 15, and 20 μs.

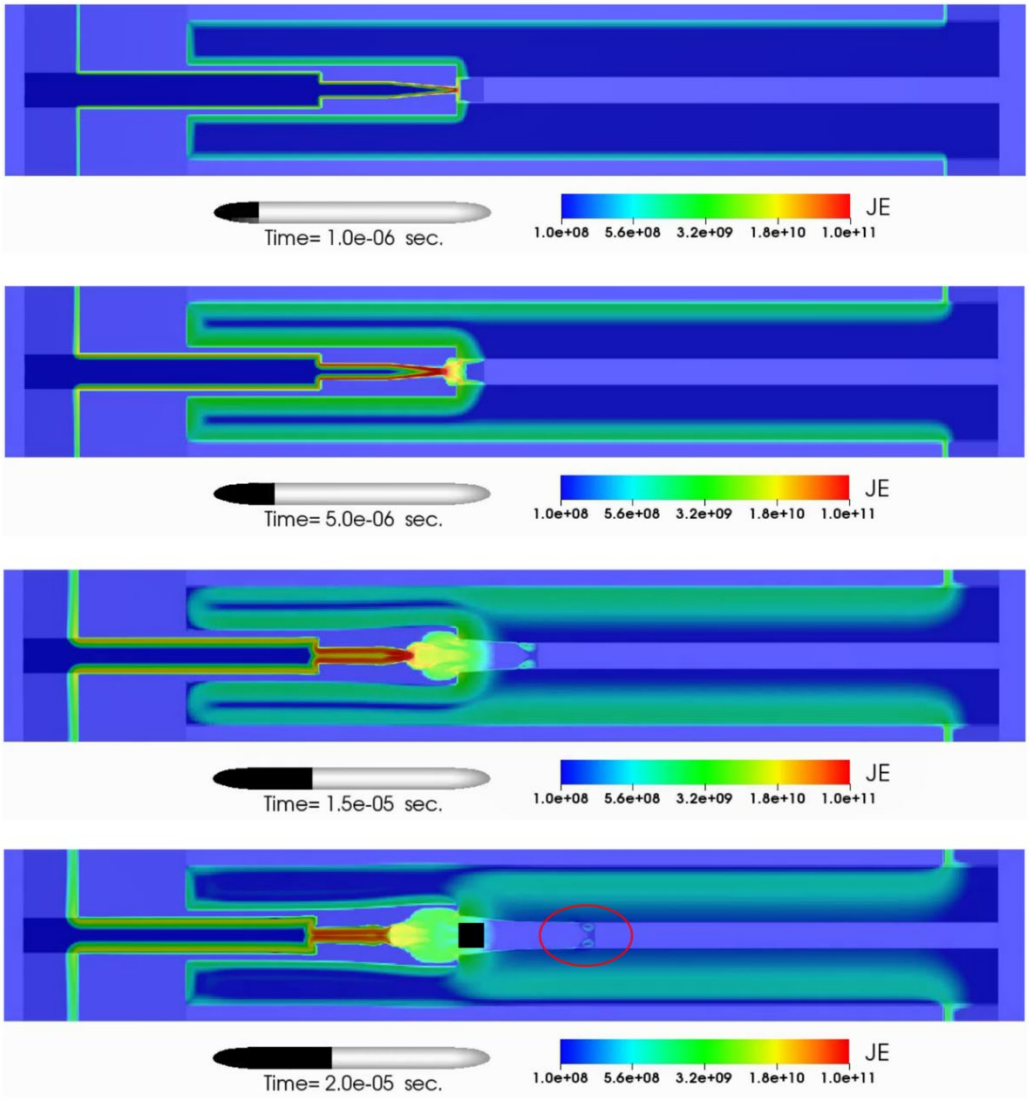

Fig. 2 ALEGRA simulations of the electrothermal gun showing the path and progression of the current density at 1, 5, 15, and 20 μs; pseudocolor of the current density is on a log scale

Observed in the simulation is the evaporation of the tip at current densities on the order of 10^{10} to 10^{11} A/m^2 followed by rapid plasma expansion in the chamber area causing a gradual deformation and outward expansion of the chamber and initial bore region of the barrel. The insulating sleeve and epoxy were replaced by a single material (polycarbonate) in the simulations for simplicity. Simulations show the insulation is initially compressed by the large pressures, opening a cavity and reducing the accelerating force on the aluminum pellet. After 6 μs, some insulation material begins to be eroded/vaporized, mixing in with the copper-vapor plasma. However, it is uncertain to what extent it contributes as a working fluid for propulsion. While the mass of the copper in the plasma is much greater, the total volume fraction of low-density insulator material in the cavity–plasma region increases throughout the launch process. For example, in the reduced-chamber design the insulator volume fraction reaches approximately 40% by 10 μs. Additionally, the simulations capture the deformation of the lower-strength barrels. Profiles of sectioned barrels from experiment match the final chamber and bore expansion of the simulation at 40 μs extremely well and scales with the yield strength of the barrel.[1,2]

Velocity had a strong dependence on barrel strength. The simulations matching the measured barrel hardness with equivalent yield strength (and thus barrel expansion) followed the velocity profile from PDV as shown in Fig. 3 with final velocity matching to within 2%. The predicted and measured current pulses are also shown in the figure for comparison. Typical peak currents are on the order of 350 kA.

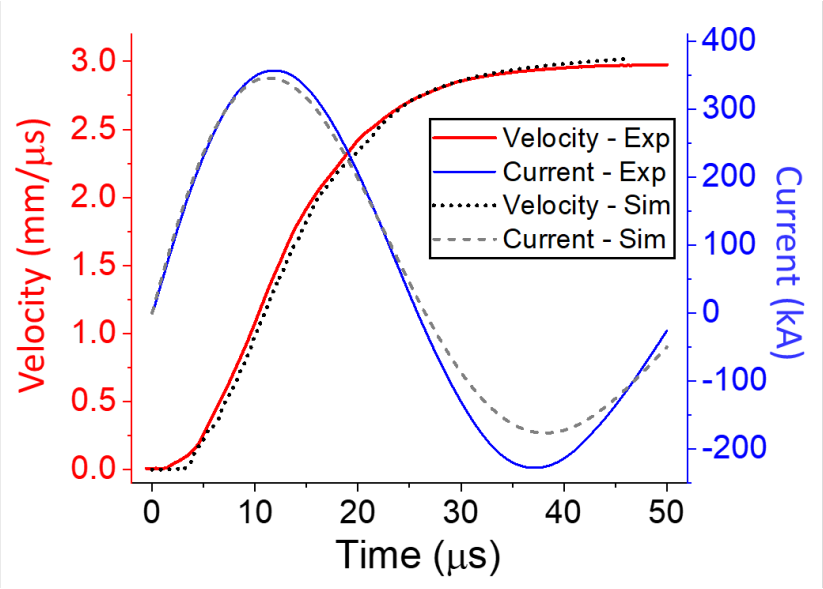

Fig. 3 Comparison of ALEGRA simulations of the standard barrel with experimentally acquired data; PDV for velocity (red) and applied current (blue)

At early times, the current density is sufficient in the projectile to cause vaporization at the back of the pellet, and some current continues with it during acceleration. Nevertheless, the current density in the pellet rapidly decreases below levels that will cause further vaporization. Yet, continued erosion in the simulations occurs. The projectile in the 20-μs simulation frame is circled in red and 48% of its mass has been lost. For comparison a black square of the original size and location of the pellet is also shown in the frame.

The simulations had a one-cell layer of air inserted between the projectile and barrel to allow free movement of the projectile. However, during acceleration the back of the projectile expands to fill the bore, creating direct contact and "welding" of the material interfaces due to the nature of Eulerian mesh. Because the aluminum pellet is much softer than the barrel, it yields along the pellet sides and the pellet accelerates smoothly. While high-speed video of experiments shows a strong plasma cloud following the projectile, which might indicate the emission of aluminum vapor from the back of the projectile, the substantial mass removed in the simulations (larger than 50% for some simulations) is not observed experimentally. A soft-captured aluminum cylinder launched at 3100 m/s had an eroded back end (see Fig. 4) and a reduction in mass from 0.24 g to 0.19 g (20%). The projectile was stopped in 1.92 m of 0.05 g/cm^3 shaving cream. The machining marks were still clearly visible on the front of the pellet, signifying that any damage to the pellet occurred during launch and not during capture. Thus, while the simulations depicted the barrel expansion and velocity very well, the velocity was not necessarily valid due to the excess erosion (and thus mass reduction) of the pellet.

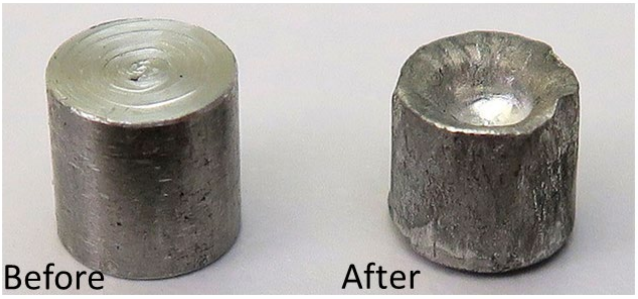

Fig. 4 Aluminum projectile prior and after launch; image shows cratering occurs at the back of the soft-captured pellet

While the initial simulations proved extremely useful in gun design, increasing both efficiency and peak velocities of the launch system, erroneous erosion of the projectile rendered them less useful for impact studies and created uncertainty in the simulation validity. Thus, several modifications were made to the simulations in order to preserve pellet integrity.

3. Modified Simulation Approach

The amount of pellet erosion was even more pronounced in hardened barrel simulations. Figure 5 shows the projectile velocity for a standard barrel design that was hardened to a yield strength of 1400 MPa with a pellet having material properties set for aluminum 7075-T6. A pseudocolor image of aluminum density just before muzzle exit shows the loss of projectile material along the barrel wall and the pellet nearly breaking apart. Artificially hardening the pellet to a strength greater than that of the barrel preserves the pellet, but friction at the projectile–bore interface stops the projectile before it exits the barrel. Methods creating multiple cell layers (up to four) of very soft material just at this interface to allow low friction motion proved unfruitful as excessive expansion of the barrel occurred for greater than one layer, slowing the projectile, while a single layer did not prevent projectile breakup.

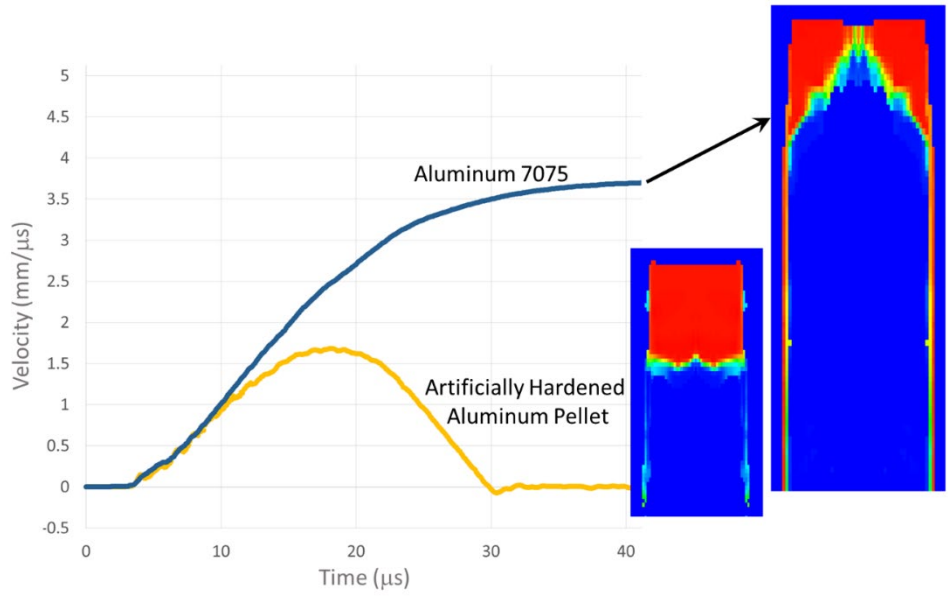

Fig. 5 Simulations of the standard barrel design with steel yield strength of 1400 MPa with velocity and density profiles for two aluminum pellets, one with aluminum 7075-T6 properties and one artificially hardened

Replacing a portion of the barrel with a frictionless mesh boundary along the length of the bore successfully corrects the excessive projectile erosion. The mesh was split into two regions. One region from 7.5 mm beyond the electrode–pellet interface (i.e., the first 7.5 mm of the bore or 1 1/2 lengths of the pellet) to the back of the electrode and hot plate was left unchanged from the previous simulations, while the mesh in the second region (beyond the 7.5 mm of barrel bore) was reduced to the diameter of the bore, as depicted in Fig. 6. Thus, the bore–projectile interface in that region was at the mesh boundary and allowed motion to occur after the initial

acceleration without Eulerian "welding". Boundary conditions were set in this region to prevent the outflow of material and maintain the pressures observed in the chamber. The ground plate was placed on the outer portion of the barrel near the chamber–bore interface, which allowed current flow similar to the experiments and previous simulations.

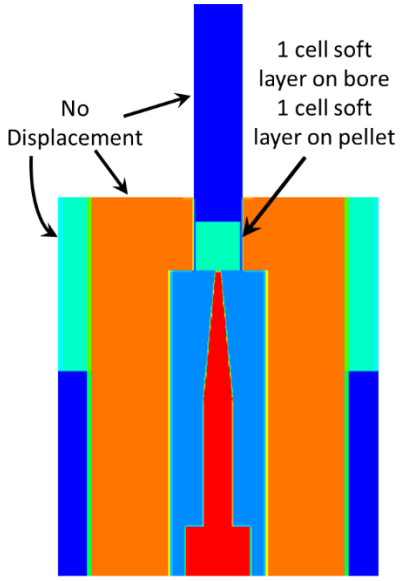

Fig. 6 Layout of the modified simulation mesh in the region of the pellet–electrode interface

The yield strength and shear modulus were then varied in an elastic–perfectly plastic model to produce pellet deformation that matched the experimentally captured pellet. A resulting 3-D isovolume of the projectile compares very favorably with the soft-captured pellet and is shown in Fig. 7a. Figure 7b shows the resulting projectile (green) with only 20% mass reduction and a comparison with the projectile from the original simulation method (black outline), both at 40 μs. The simulated pellets shown have a yield strength and shear modulus double that of the standard 7075-T6 aluminum used in the experiment, to match the electrically eroded crater depth at the back of the pellet and the slight erosion along the sides. The isovolume is somewhat inaccurate at the "tail" of the projectile, showing material at larger diameters than the original pellet diameter. Figure 8 shows the temperature of the projectile material for a simulation of the reduced-chamber barrel design at 10, 20, and 32 μs. The temperature profiles indicate the material in the expanded region at the back of the projectile is melted and would not be present in the final state, just as the soft-captured particle evidence suggests.

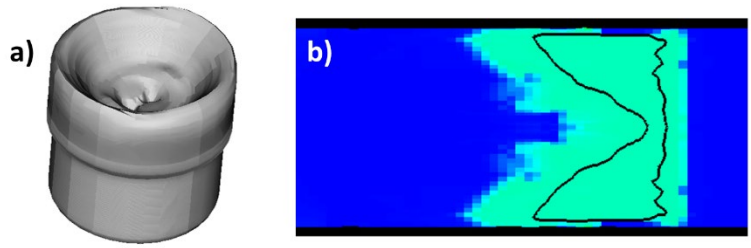

Fig. 7 Projectile shape resulting from modified ALEGRA simulations as a) 3-D isovolume and b) 2-D slice comparing the block suppression simulation (green) and original simulation (black outline)

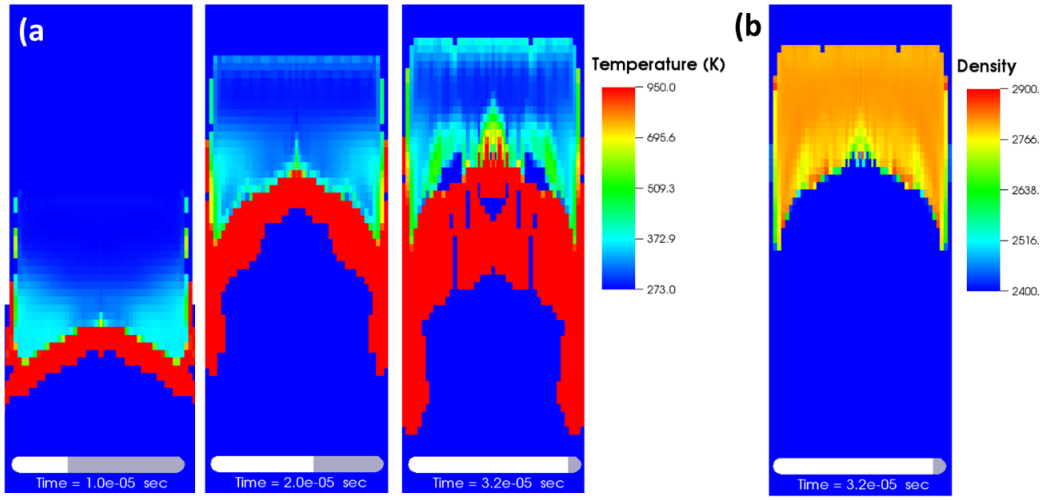

Fig. 8 a) Projectile temperature and b) clipped density to show only solid material for simulations of the reduced-chamber barrel design

Aluminum vapor is also observed trailing the projectile in the simulations (not distinguished from liquid in Fig. 8a due to the temperature clip), reinforcing observations from high-speed video. The aluminum density shown in Fig. 8b is clipped to show only solid material and render a better image of what the projectile's final state would be if soft captured. Simulations using aluminum strength parameters from one to two times that of 7075-T6 aluminum had fairly similar results with baseline 7075-T6 aluminum still slightly overeroding and double the strength, producing nearly identical cratering (1.4-mm depth in the experimentally captured pellet).

In the simulations, a single artificially softened cell layer for each material was inserted at the steel-bore–projectile interface to reduce friction during the initial acceleration before the pellet reached the reduced-block region of the mesh. This region coincides with cavity expansion (especially in the softer barrels). In the original simulations, barrel expansion was determined to have a direct effect on the

projectile velocity. Thus, this metric is also critical for the modified simulations using the suppressed block. A direct comparison between the original simulations that matched the measured barrel deformations extremely well and the suppressed-block simulations is shown in Fig. 9. In this case the bore–projectile interface region was reduced to 5 mm (the length of the pellet) as any observed differences would be amplified with the shorter region. The original simulation is overlaid on the modified simulation using a black outline. At 30 μs the barrel expansion is complete. While expansion occurs farther down the bore in the original simulations because the no-displacement boundary conditions do not allow it in the modified simulations, greater expansion in the initial pellet-position area occurs in the modified simulations. This is a direct result of having the large pressures occur at the artificial "end" of the steel barrel instead of closer to the center. These two volumes nearly balance out and the resulting velocity still matches the experimentally determined value (see Fig. 10). For the hardened barrels in the reduced-chamber design, this is not an issue of concern because of the very small deformations.

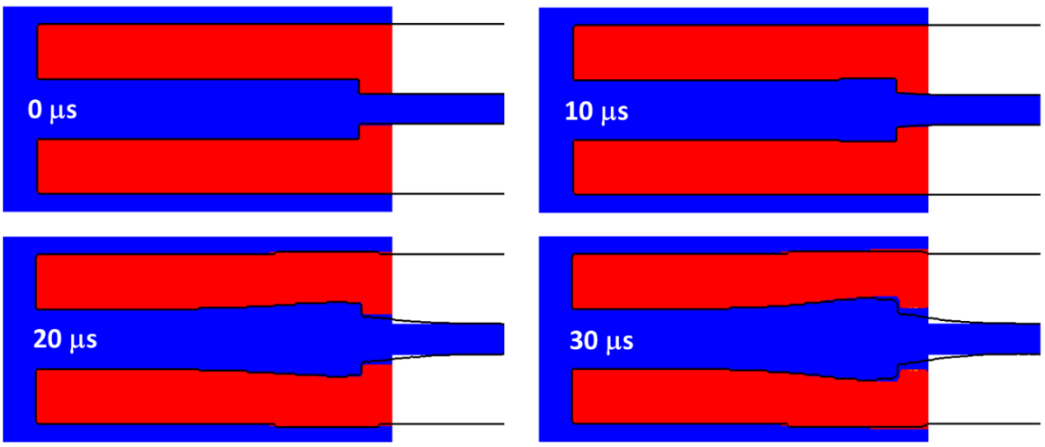

Fig. 9 Barrel expansion in original ALEGRA simulations (black outline) compared with simulations with the suppressed block in the bore region of the barrel (color) at 0, 10, 20, and 30 μs.

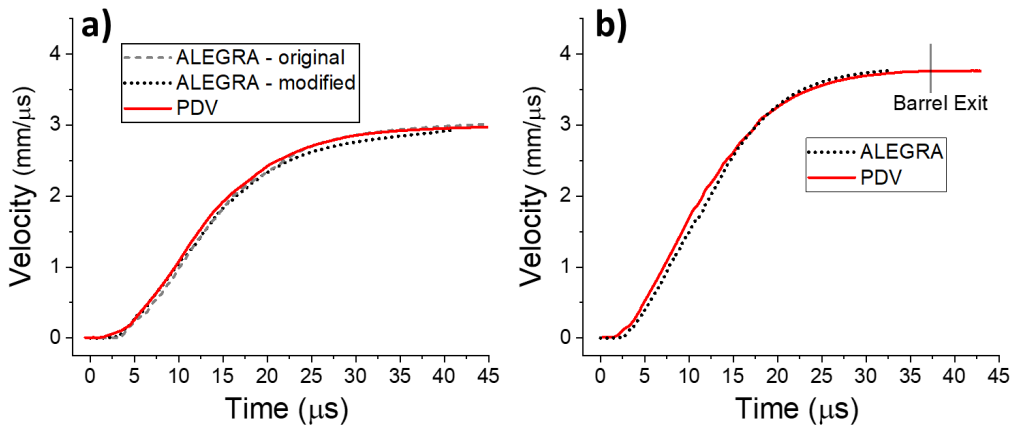

Fig. 10 Velocity-profile comparisons to PDV for a) the standard barrel with original and modified ALEGRA simulations and b) the reduced-chamber barrel design with the modified ALEGRA simulations

While the modified ALEGRA simulations do not follow the PDV results as closely as the original simulations of the standard barrel design, the final velocity and barrel exit are still within 2% of experiment (2930 m/s vs. average experimental peak velocity of 2988 m/s). Additionally, the pellet is intact and the correct mass. Figure 10b shows the PDV results for a nominal shot using the reduced-chamber barrel design compared with the modified ALEGRA simulation results. (In order to reduce simulation time, the bore region of the barrel was reduced to 80 mm; thus, the simulation ends at 33 μs, 4.5 μs before barrel exit in experiment, marked with a grey vertical line.) Based on an extrapolation of the data, the velocity at exit of a 100-mm bore simulation would be 3875 ± 25 m/s compared with an average peak velocity of 3851 ± 102 m/s experimentally. Because the velocity is dependent on the system inductance and energy delivered to the gun mount, variation in peak velocities occurs. While no attempt was made to match individual shots with the simulations, the predicted velocity for the reduced-chamber barrel design was within 1% of two of the measured PDV results and within 5% for the other three for the five launches attempted with that design and electrode configuration.

4. Conclusions

An electrothermal gun was designed and attained hypervelocities for impact studies. Guidance resulting from benchmarked simulations using the ALEGRA hydrocode with MHD led to significant projectile velocity gains. While the initial simulations reproduced and predicted the velocity profiles and barrel expansion extremely well, significant erosion of the projectile occurred in the simulations that was not observed in the experiments. This was a direct result of Eulerian "welding" at the projectile–barrel interface. Modifications including block suppression in the

region of the barrel downstream of the chamber and the electric action allowed the acceleration observed experimentally, while preserving projectile integrity, thus overcoming the erroneous erosion issues and proving to be a useful tool in predictive ballistic capabilities.

5. References

1. Bartkowski P, Berning P, Uhlig C, Coppinger MJ. Electrical arc driven hypersonic projectiles. Aberdeen Proving Ground (MD): Army Research Laboratory (US); 2019 Apr. Report No.: ARL-TR-8683.

2. Uhlig WC, Berning PR, Bartkowski PT, Coppinger MJ. Electrically-launched mm-sized hypervelocity projectiles. Int J Imp Eng. 2020;137:103441.

3. Robinson AC, Brunner TA, Carroll S, Drake R, Garasi CJ, Gardiner T, Haill T, Hanshaw H, Hensinger D, Labreche D, et al. ALEGRA: an arbitrary Lagrangian-Eulerian multimaterial, multiphysics code. Proceedings of the 46th AIAA Aerospace Sciences Meeting; 2008 Jan 7–10; Reno, NV. Paper No.: AIAA-2008-1235.

4. Rott M. The LRT/TUM small caliber electrothermal accelerator. IEEE Trans Magn. 1993;29(1).

5. Yoshida H, Hoshi Y, Uematsu K, Kitazawa Y. A single, small particle launch system by electrothermal gun and microsabot. Rev Sci Inst. 1997;68:178.

6. Fair HD. Progress in electromagnetic launch science and technology. IEEE Trans Magn. 2007;43(1).

7. Lee T, Taber G, Vivek A, Daehn GS. Characterization of high-speed flyer evolution by multi-probe photon Doppler velocimetry. Paper presented at: ICHSF 2018. 8th International Conference on High Speed Forming; 2018 May 13–16; Columbus, OH.

8. Pastore R, Podlesak T, Singh H. Progress in 2N megajoule electrothermal-chemical gun pulser. Proceedings of the 9th IEEE International Pulsed Power Conference; 1993. p. 783–786.

9. Katulka GL, DelGuercio M, Pastore R, Singh D, Burdalski RJ. A 4-MJ mobile pulse power facility for electrothermal-chemical gun research. Proceedings of the 10th IEEE International Pulsed Power Conference; 1995; Albuquerque, NM. Vol. 1, p. 267–272.

10. Uhlig WC, Heine A. Electromagnetic diagnostic techniques for hypervelocity projectile detection, velocity measurement, and size characterization: theoretical concept and first experimental test. J Appl Phys. 2015;118:184901.

11. Uhlig WC, Hummer CR. In-flight conductivity and temperature measurements of hypervelocity projectiles. Procedia Eng. 2013;58:48–57.

12. Strand OT, Goosman DR, Martinez C, Whitworth TL, Kuhlow WW. Compact system for high-speed velocimetry using heterodyne techniques. Rev Sci Instrum. 2006;77(8):1–9.

13. Voth T, Mosso S. An eXtended Finite Element/Eulerian (XFEM/Eulerian) approach for solid mechanics. Albuquerque (NM): Sandia National Laboratory (US); 2012. Report No.: SAND2012-3070C.

List of Symbols, Abbreviations, and Acronyms

2-D	2-dimensional
3-D	3-dimensional
CCDC	US Army Combat Capabilities Development Command
L/D	length-to-base-diameter ratio
MHD	magnetohydrodynamic
PDV	Photon Doppler Velocimetry

1 (PDF) DEFENSE TECHNICAL INFORMATION CTR DTIC OCA

1 (PDF) CCDC ARL FCDD RLD CL TECH LIB

35 (PDF) CCDC ARL FCDD RLW R FRANCART S SCHOENFELD FCDD RLW PA S BILYK J FLENIKEN T KOTTKE M MCNEIR C WOLFE P BERNING M COPPINGER W UHLIG L VANDERHOEF A VALENZUELA B WILMER FCDD RLW PC J CAZAMIAS S SEGLETES R BECKER D CASEM FCDD RLW PD M KEELE F MURPHY C RANDOW D KLEPONIS A BARD N BRUCHEY S SCHRAML R MUDD R DONEY G VUNNI M ZELLNER FCDD RLW PE P SWOBODA P BARTKOWSKI D GALLARDY D HORNBAKER K KRAUTHAUSER FCDD RLW PF N GNIAZDOWSKI FCDD RLW PB C HOPPEL

6 (PDF) US ARMY TACOM J WHITE L FRANKS D TEMPLETON M LAWSON J HITCHCOCK N COOPER

3 (PDF) PM ABCT J ROWE E BARSHAW R NICOL

4 (PDF) NATL GROUND INTLLGNC CTR D EPPERLY T SHAVER T WATERBURY D DOBROWOLSKI

1 (PDF) PM MRAP J PEREZ (JPO)

1 (PDF) DARPA/DSO L CHRISTODOULOU

1 (PDF) PM BFVS D SPENCER

1 (PDF) NSWC CARDEROCK DIV R PETERSON

2 (PDF) SANDIA NATL LAB E STRACK J NIEDERHAUS

2 (PDF) BAE SYSTEMS LANDS & ARMAMENTS R APPLETON

1 (PDF) GDLS M KAUTZER

1 (PDF) US ATEC E SANDERSON